

CHAPTER 2

Synthesis and Characterization of Cerium (IV) and Thorium (IV) Phosphates

2.1 INTRODUCTION

Synthesis and characterization constitute the most essential aspects of materials research. A combination of the two, leads to the preparation of tailor made materials, to perform a specific function with desired properties. The interest in novel materials with predictable structures and properties for specific applications has given rise to the development of a variety of preparation methodologies. The method chosen for any material preparation, depends not only on the material composition, but also on the form in which it is required for a specific application.

The present study deals with the synthesis and characterization of amorphous metal phosphates of the class of TMA salts,

a) **Cerium (IV) Phosphate (CP)**

b) **Thorium (IV) Phosphate (TP)**

2.2 LITERATURE SURVEY IN THE CURRENT AREA OF STUDY

A variety of CPs have been reported in accordance with preparation methods and the reaction conditions [1-3]. CP gels with P/Ce ratios of 1.25-1.50 were synthesized by Hartley in 1882[4], and observed to yield acidic solutions when placed in water. A systematic study of these gels was not attempted until the work of Cilley and Larsen [5,6]. They prepared gels having ratios of P/Ce ranging from 0.55 to 1.53, and observed that these gels exhibited ion exchange characteristics. Equilibrating a gel (P/Ce = 1.48) with alkali cations in a pH 5 solution for two weeks yielded exchange capacities of 1.44 meq Li⁺/g of solid and 1.66 meq/g Na⁺ and K⁺. Subsequently crystalline CPs [2,3] and cerium(IV) phosphate-sulfates [7-10] were prepared and their ion exchange properties examined. Cerium orthophosphates CePO₄ and CePO₄·0.5H₂O, metaphosphate Ce(PO₃)₂ and ultraphosphate CeP₅O₁₄, with trivalent CPs, while cerium diphosphate Ce₂PO₇, metaphosphate Ce(PO₃)₄ and hydrogenphosphates Ce(HPO₄)₂·nH₂O (n=0, 0.33, 1.33 and 3) with tetravalent CPs have been reported [11].

A variety of crystalline CPs, Ce(HPO₄)₂·nH₂O have been reported by the reaction of ceric sulfate (Ce(SO₄)₂·8H₂O) and H₃PO₄. It is observed that the structures varied according to the reaction conditions: P/Ce ratio, concentration of H₃PO₄, reaction temperature, digestion time and humidity [1-3, 11].

Hikichi et al [12] prepared monazite-type CePO_4 by heating $\text{CePO}_4 \cdot 0.5\text{H}_2\text{O}$ and reported a high sintered density (99%) at 1500 °C. Another approach to synthesize CP was through the reaction between rare earth salts and ammonium phosphate [13,14].

Rajesh et al [15] have reported synthesis of nano-size CP by sol-gel process involving electrostatic stabilization and gelation in ammonia atmosphere. This can be used for applications related to catalysis, coatings, and low-temperature densification, and for synthesis of nano-composites and nano-size particles.

Recently, a mechano-chemical method has also been used to synthesize rhabdophane-type CePO_4 , by grinding $\text{Ce}(\text{NO}_3)_3 \cdot 6\text{H}_2\text{O}$, $\text{CeCl}_3 \cdot 7\text{H}_2\text{O}$ and $\text{Ce}(\text{CO}_3) \cdot 7\text{H}_2\text{O}$ along with $(\text{NH}_4)_2\text{HPO}_4$ [16].

Synthesis of microcrystalline CP, using $\text{Ce}(\text{NO}_3)_3 \cdot 6\text{H}_2\text{O}$ and H_3PO_4 , in ethanolic media was reported by Bao et al [17].

Crystalline cerium (IV) phosphate-hydrogenphosphate hydrate $\text{Ce}_2(\text{PO}_4)_2(\text{HPO}_4) \cdot \text{H}_2\text{O}$ was also synthesized from $(\text{NH}_4)_2\text{Ce}(\text{NO}_3)_6$ and H_3PO_4 acid solution in autoclave and in polytetrafluoroethylene (PTFE) closed containers at 150°C [18].

Shakshooki et al have reported synthesis of poly (vinylalcohol)/fibrous cerium phosphate ($\text{Ce}(\text{HPO}_4)_2 \cdot 2.9\text{H}_2\text{O}$) nano-composite membranes of different weight percentages [19]. Synthesis and formation mechanism of monoclinic CePO_4 nano-wires prepared by a hydrothermal method has been reported by Ekthammathat [20].

Nazaraly and Wallez have reported synthesis of $\text{Ce}(\text{PO}_4)(\text{HPO}_4)_{0.5}(\text{H}_2\text{O})_{0.5}$ from CeO_2 , H_3PO_4 hydrothermally [21].

Hanna et al have reported synthesis of CePO_4 , nano-particles with hexagonal or monoclinic phase by the reaction between $\text{Ce}(\text{SO}_4)_2 \cdot 4\text{H}_2\text{O}$ and two different phosphate sources H_3PO_4 and Na_2HPO_4 . The gel obtained was dried and calcined at different temperatures (200, 400 and 800 °C) [22].

Several series of metal-thorium phosphates of general formulae $\text{MTh}_2(\text{PO}_4)_3$ (M= alkali, alkaline and transition metals) have been reported where all these phosphates were obtained from mixture of thorium oxide, metal carbonate and $\text{NH}_4\text{H}_2\text{PO}_4$ using dry chemistry methods and also by a co-precipitation process [23].

Brandel et al have reported synthesis of amorphous TP by precipitation from thorium salts and H_3PO_4 (formulated as $\text{Th}(\text{PO}_4)_2(\text{HPO}_4) \cdot n\text{H}_2\text{O}$; $n=3-7$) [24].

Alberti et al have synthesized amorphous TP at room temperature by mixing an acidic solution of a thorium salt with a solution of phosphoric acid [2].

Wallez et al [25] have prepared crystallized precursor thorium phosphate hydrogenphosphate hydrate $\{\text{Th}(\text{PO}_4)_4(\text{HPO}_4)_2 \cdot 2\text{H}_2\text{O}\}$ by the precipitation of a stoichiometric mixture of concentrated ThCl_4 solution with 5 M H_3PO_4 in a closed container which was then heated to 1050-1250 °C. Several attempts are based on the direct precipitation and evaporation (solid state reaction – wet chemistry route) of a mixture of $\text{Th}(\text{NO}_3)_4 \cdot 4\text{H}_2\text{O}$ and concentrated H_3PO_4 .

Laud and Hamell reported the chemical formula $\text{Th}_3(\text{PO}_4)_4$, for a phase obtained up to 1500 °C by reaction between ThO_2 and Na_2HPO_4 [26].

Tananaev [27] has extensively studied synthesis of various kinds of TPs (hydrated and non-hydrated), starting from aqueous mixture of $\text{Th}(\text{NO}_3)_4 \cdot 8\text{H}_2\text{O}$ and Na_2HPO_4 .

A K De et al [28] have synthesized TP polymers using $\text{Th}(\text{NO}_3)_4 \cdot 4\text{H}_2\text{O}$ and H_3PO_4 under different conditions. The P/Th ratio of the samples varied from 1.69 to 2.1.

Rawat et al [29] have prepared crystalline $\text{Th}_2(\text{PO}_4)_2(\text{HPO}_4) \cdot \text{H}_2\text{O}$ by addition of aqueous solution of $\text{Th}(\text{NO}_3)_4 \cdot 4\text{H}_2\text{O}$ and $\text{NH}_4\text{H}_2\text{PO}_4$. Crystalline $\text{Th}_2\text{P}_3\text{HO}_{12}$, was prepared by heating $\text{Th}_2(\text{PO}_4)_2(\text{HPO}_4)$ at 500 K under flowing argon gas. Crystalline $\alpha\text{-Th}_4\text{P}_6\text{O}_{23}$ and $\beta\text{-Th}_4\text{P}_6\text{O}_{23}$ were also prepared by heating crystalline $\alpha\text{-Th}_4(\text{PO}_4)_4\text{P}_2\text{O}_7$ and $\beta\text{-Th}_4(\text{PO}_4)_4\text{P}_2\text{O}_7$ respectively at 1000 K for 24 h under flowing argon gas.

Varshney et al have reported synthesis, characterization and application of fibrous CPs and TPs as cation exchangers [30-34].

2.3 MATERIAL SYNTHESIS

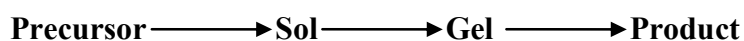
Presently, soft chemistry routes involving low temperatures, popularly known as “Chimie Douce” by the French, are fast replacing the traditional ceramic (Brute force) methods. The traditional ceramic method involves mixing and grinding powders of the constituents as oxides, nitrates, sulphates, chlorides or carbonates and heating them at high temperatures and high pressures with intermediate grinding, mixing and rapid quenching. The present day trend is to avoid brute force methods in order to get a better control of the structure at molecular level, stoichiometry and

phasic purity. Low temperature chemical routes and reactions which involve mild conditions are of great interest and more preferred because of the ensuing energy savings.

In the present study CP and TP have been synthesized by sol-gel route that represents the most essential component of soft chemistry routes.

Sol-gel Process

The sol-gel process is a wet-chemical technique for the fabrication of materials, employing low temperature, starting either from a chemical solution or colloidal particles (sol for solution or nano-scale particle) to produce an integrated network (gel). In general, sol-gel technique can be regarded as the preparation of the sol, gelation of the sol and removal of the solvent. The overall sol-gel process can be represented by the following sequence of transformations [35]:



Precursors are starting materials, in which the essential basic entities for further network formation are present in the correct stoichiometry. Typical precursors are metal alkoxides and metal chlorides.

Sol is a colloidal suspension of particles in a liquid, the particles typically ranging from 1-100 nm in diameter.

Gel is a semi-rigid solid, in which solvent is contained in a network/framework of the material, which is either colloidal (essentially a concentrated sol) or polymeric.

The name “sol-gel” is thus given to the process, because of the distinctive viscosity increase that occurs at a particular point in the sequence of steps. A sudden increase in viscosity is the common feature in sol-gel processing, indicating the onset of gel formation. Sol-gel process can be distinguished from precipitation by its specific property to stabilize a finely dispersed (mostly colloidal) phase in solution.

Typically, formation of a metal oxide involves connecting the metal centres with oxo (M-O-M) or hydroxo (M-OH-M) bridges, therefore generating metal-oxo or metal-hydroxo polymers in solution. The drying process serves to remove the liquid phase from the gel, thus forming a porous material, and then a thermal treatment (firing) may be performed in order to favour further polycondensation and enhance mechanical properties.

Important steps involved in sol-gel synthesis are –

Hydrolysis: It involves reaction of inorganic or organometallic precursor with water or a solvent, at ambient or slightly elevated temperature. Acid or base catalysts are added to speed up the reaction.

Polymerization: This step involves condensation of adjacent molecules wherein water/alcohol is eliminated and metal oxide linkages are formed. Polymeric networks grow to colloidal dimensions in the liquid (sol) state.

Gelation: It leads to the formation of a three dimensional network throughout the liquid, by the linking up of polymeric networks.

Aging: Aggregation of smaller polymeric units to the main network progressively continues on ageing the gel. A continuous change in structure and properties of a completely immersed gel in liquid is called ageing. Solvent molecules however, remain inside the pores of the gel.

Drying: Here, solvent is removed at moderate temperatures ($< 200\text{ }^{\circ}\text{C}$) leaving the residue behind.

Dehydration: This step is carried out between $400\text{ }^{\circ}\text{C}$ and $800\text{ }^{\circ}\text{C}$ to drive off the organic residues and chemically bound water.

Densification: Heating the porous gel at high temperatures, leads to formation of a dense oxide product. The densification temperature depends considerably on the dimensions of the pore network, the connectivity of the pores, and surface area.

The sol-gel method, thus offers the possibility to prepare solids with pre-determined structure by varying the experimental conditions such as the choice of reagents, concentration, mode and rate of mixing, temperature, pH, ageing and drying conditions. Amongst the parameters varied in sol-gel routes, microwave (MW) irradiation has made a huge impact lately. Currently, it is used extensively in organic synthesis as well as materials processing. MWs penetrate materials (absorption of heat entirely through the material) which results in even and rapid heating, further heating is controlled and more precise than conventional heating. Thus, MW irradiation is considered as a catalyst for chemical reactions. MWs interact directly with molecules to generate heat thus no liquid medium is required as in conventional heating. It is thus considered as an environment friendly technology as it can reduce or even eliminate use of solvents. In short, MWs act as catalyst producing heat that is rapid, even/uniform, controlled heat which produces purer products, eliminates use of solvents and is environment friendly in nature. [36-38].

In sol-gel synthesis, variation in any of these parameters mentioned above yields materials with different characteristics. The preparation procedure thus affects the composition and structure, which is further reflected in the properties/performance such as porosity, surface acidity and crystallinity.

Advantages of Sol-Gel Process

- ❖ High homogeneity –due to intimate mixing of raw materials
- ❖ High purity
- ❖ Low temperature processing (energy savings, minimize evaporation losses, minimize air pollution, no reaction with container)
- ❖ More uniform phase distribution in multicomponent systems
- ❖ Materials with improved and desired properties (tailor made materials) can be obtained
- ❖ Porous materials using templates

Disadvantages of the Sol-Gel Process

- ❖ Large shrinkage during processing
- ❖ Residual fine pores
- ❖ Residual hydroxyl groups when hydroxides are used
- ❖ Residual carbon (originating from templates)
- ❖ Health hazards of organic solvents
- ❖ Long processing times

2.4 EXPERIMENTAL

Materials: Thorium Nitrate ($\text{Th}(\text{NO}_3)_4 \cdot 5\text{H}_2\text{O}$), Ceric Sulphate ($\text{Ce}(\text{SO}_4)_2 \cdot 4\text{H}_2\text{O}$) and Sodium dihydrogen phosphate ($\text{NaH}_2\text{PO}_4 \cdot 2\text{H}_2\text{O}$) were procured from Loba Chemicals, Mumbai. Deionized water (DIW) was used for all the studies. Microwave irradiation was carried out using microwave reactor (Milestone- Start Synth Microwave Synthesis Labstation; installed and delivered microwave power = 1200 watts, controlled via microprocessor in 1 watt increments).

2.4.1 Synthesis of Cerium Phosphate (CP) and Thorium Phosphate (TP)

The main objective in the synthesis of CP and TP, was to obtain materials with high ion exchange capacity. As indicated earlier in the text, in sol-gel method of synthesis, several parameters are varied to achieve this objective. Several sets of materials were prepared varying conditions in each case using cation exchange

capacity (CEC) as the indicative tool. **Tables 2.1 and 2.2** describe optimization of reaction parameters for synthesis of CP and TP respectively.

Synthesis of CP at optimized condition: A solution containing $\text{Ce}(\text{SO}_4)_2 \cdot 4\text{H}_2\text{O}$ [0.1M, 50 mL in 10% (w/v) H_2SO_4] was prepared, to which $\text{NaH}_2\text{PO}_4 \cdot 2\text{H}_2\text{O}$ [0.3M, 50 mL] was added dropwise (flow rate $1 \text{ mL} \cdot \text{min}^{-1}$) with continuous stirring for an hour at room temperature, when gelatinous precipitates were obtained (Step-I). The resulting gelatinous precipitate was allowed to stand for 3 h at room temperature, then filtered, washed with DIW to remove adhering ions and dried at room temperature (Step-II).

Synthesis of TP at optimized condition: An aqueous solution of $\text{Th}(\text{NO}_3)_4 \cdot 5\text{H}_2\text{O}$ [0.1M, 50mL] was added drop wise (flow rate $1 \text{ mL} \cdot \text{min}^{-1}$) to an aqueous solution of $\text{NaH}_2\text{PO}_4 \cdot 2\text{H}_2\text{O}$ [0.2M, 100 mL] with continuous stirring for an hour at room temperature, when gelatinous precipitates were obtained (Step-I). The resulting gelatinous precipitate was allowed to stand for 5 h at room temperature, then filtered, washed with DIW to remove adhering ions and dried at room temperature (Step-II).

Synthesis of CP and TP under microwave irradiation: CP and TP have also been synthesized under microwave irradiation to yield CP_M and TP_M , where gelatinous precipitate obtained in step-I was subjected to microwave irradiation for optimum time and temperature (**Table 2.3**), then filtered, washed with DIW to remove adhering ions and dried at room temperature (Step-II).

Acid treatment: The above materials obtained in step-II were broken down to the desired particle size [30-60 mesh (ASTM)] by grinding and sieving. 5 g of this material was treated with 50 mL of 1 M HNO_3 for 30 min with occasional shaking. The material was then separated from acid by decantation and treated with DIW to remove adhering acid. This process (acid treatment) was repeated at least 5 times. After final washing, the material was dried at room temperature. These materials were used for all studies.

Chapter 2 - Synthesis and Characterization of CP and TP

Table 2.1 Varying reaction parameters for synthesis of Cerium Phosphate (CP)

| Parameters varied | No | Concentration M : A (M) | Volume M : A (mL) | pH | Temp. (±2 °C) | Stirring Time | Aging Time | CEC meq/g |
|-------------------|-----------|-------------------------------|-------------------------|----------|------------------|------------------|---------------|--------------|
| Concentration | 1 | 0.1 : 0.1 | 50 : 50 | 6 | 34 | 1 hr | 15 hr | 2.01 |
| | 2 | 0.1 : 0.2 | 50 : 50 | 5.5 | 34 | 1 hr | 15 hr | 2.13 |
| | 3 | 0.1 : 0.3 | 50 : 50 | 5 | 34 | 1 hr | 15 hr | 2.38 |
| Volume | 4 | 0.1 : 0.2 | 50 : 100 | 5.5 | 34 | 1 hr | 15 hr | 1.89 |
| | 5 | 0.1 : 0.2 | 100 : 50 | 5.5 | 34 | 1 hr | 15 hr | 1.24 |
| | 6 | 0.1 : 0.3 | 50 : 100 | 6 | 34 | 1 hr | 15 hr | 1.80 |
| | 7 | 0.1 : 0.3 | 100 : 50 | 6 | 34 | 1 hr | 15 hr | 1.34 |
| Temperature | 8 | 0.1 : 0.3 | 50 : 50 | 5 | 70 | 1 hr | 1 hr | 1.47 |
| | 9 | 0.1 : 0.3 | 50 : 50 | 5 | 34 | 1 hr | 1 hr | 2.30 |
| Aging Time | 10 | 0.1 : 0.3 | 50 : 50 | 5 | 34 | 1 hr | 3 hr | 2.45* |
| | 11 | 0.1 : 0.3 | 50 : 50 | 5 | 34 | 1 hr | 5 hr | 2.40 |
| Stirring Time | 12 | 0.1 : 0.3 | 50 : 50 | 5 | 34 | 2hr | 3 hr | 2.40 |
| pH | 13 | 0.1 : 0.3 | 50 : 50 | 1 | 34 | 1hr | 3 hr | 2.40 |

Table 2.2 Varying reaction parameters for synthesis of Thorium Phosphate (TP)

| Parameters varied | No | Concentration M : A (M) | Volume M : A (mL) | pH | Temp. (±2 °C) | Stirring Time | Aging Time | CEC meq/g |
|-------------------|-----------|-------------------------------|-------------------------|----------|------------------|------------------|---------------|--------------|
| Concentration | 1 | 0.1 : 0.1 | 50 : 50 | 6 | 34 | 1 hr | 15 hr | 1.25 |
| | 2 | 0.1 : 0.2 | 50 : 50 | 6 | 34 | 1 hr | 15 hr | 1.30 |
| | 3 | 0.1 : 0.3 | 50 : 50 | 5.5 | 34 | 1 hr | 15 hr | 1.36 |
| Volume | 4 | 0.1 : 0.2 | 50 : 100 | 6 | 34 | 1 hr | 15 hr | 1.42 |
| | 5 | 0.1 : 0.2 | 100 : 50 | 6 | 34 | 1 hr | 15 hr | 1.35 |
| | 6 | 0.1 : 0.3 | 50 : 100 | 6 | 34 | 1 hr | 15 hr | 1.40 |
| | 7 | 0.1 : 0.3 | 100 : 50 | 5.5 | 34 | 1 hr | 15 hr | 1.34 |
| Temperature | 8 | 0.1 : 0.2 | 50 : 100 | 6 | 70 | 1 hr | 1 hr | 1.41 |
| | 9 | 0.1 : 0.2 | 50 : 100 | 6 | 34 | 1 hr | 1 hr | 1.39 |
| Aging Time | 10 | 0.1 : 0.2 | 50 : 100 | 6 | 34 | 1 hr | 3 hr | 1.45 |
| | 11 | 0.1 : 0.2 | 50 : 100 | 6 | 34 | 1 hr | 5 hr | 1.48* |
| Stirring Time | 12 | 0.1 : 0.1 | 50 : 100 | 6 | 34 | 2hr | 5 hr | 1.42 |
| pH | 13 | 0.1 : 0.1 | 50 : 100 | 1 | 34 | 1hr | 5 hr | 1.36 |

M= Metal; A=Anion; *Optimum condition

Table 2.3 Optimization of microwave irradiation for synthesis of CP_M and TP_M

| Experimental Conditions | | CEC meq·g ⁻¹ | |
|--|-------------------------|-------------------------|-----------------|
| | | CP _M | TP _M |
| Conventional method (Room Temperature ~30°C) | | 2.45 | 1.45 |
| Microwave irradiation (350-400 Watt) | 60°C for 8 min | 2.52 | 1.68 |
| | 80°C for 8 min | 2.56 | 2.14 |
| | 100°C for 8 min | 2.65 | 2.30 |
| | 120°C for 8 min | 2.70 | 2.29 |
| | 100°C for 15 min | 2.90 | 2.41 |
| | 100 °C for 20 min | 2.92 | 2.45 |

2.5 MATERIAL CHARACTERIZATION

Metal phosphates, CP and TP were subjected to physico-chemical, ion exchange characterization, instrumental methods of characterization and catalyst characterization.

2.5.1 Physico-chemical Characteristics

Physico-chemical characteristics include appearance, percentage moisture content, particle size, apparent density, true density, nature of exchanger and chemical stability (Tables 2.4 and 2.5).

Appearance: The material was observed for physical appearance such as colour, opacity/transparency, hardness etc.

CP was obtained as yellow hard granules while TP was obtained as white hard granules.

% Moisture content: Percentage moisture content of an exchanger is the ability of the exchanger to hold moisture, and depends on the matrix structure - functional groups/ionogenic groups present in the exchanger.

For determining percentage moisture content, 1 g of the material was allowed to stand in DIW for 24 h. The material was then filtered and dried at room temperature to remove surface moisture and weighed. This material was then dried at 110 °C for 4 h and reweighed after cooling in a desiccator. The percentage moisture content was calculated using the formula,

$$\% \text{ Solid} = \frac{\text{Weight of dried material}}{\text{Weight of material before drying}} \times 100 \quad (\text{Eq. 2.1})$$

$$\% \text{ Moisture content} = 100 - (\% \text{ solid}) \quad (\text{Eq. 2.2})$$

Particle size: Ion exchange materials in general, are supplied as small round beads, having a diameter between 0.3 and 1.2 mm. Large beads are preferred for pressure drop advantage in column operations. However, large beads are subject to a greater rate of breakage than those having a smaller size. The most efficient ion-exchange processes occur when most of the functional groups can be accessed (equilibrated) within a short contact time between liquid and exchanger. The larger the particle size, the greater is the time required to access groups deeper in the particles. Thus, ion exchange rate will increase as the particle size decreases. The diffusion path lengths of the exchanging ions to exchanger and from the exchanged sites to electrolyte media are shorter with smaller particle sizes [39, 40].

In the present study, CP and TP of particle size 0.25–0.59mm [30-60 mesh (ASTM)] were used.

Density and specific gravity: Density is characteristic of the exchanger. Most common of these is the **apparent density** or *bulk density* or *column density* in which the weight of the ion exchanger per unit volume is determined. Density is used to measure the performance of an ion exchanger in commercial units. A change in density after extended use is a signal that chemical degradation has occurred.

Specific gravity generally refers to the value determined for wet exchanger when using a pycnometer. This is also known as **true density**. Cation exchangers have a greater specific gravity than anion exchangers. To avoid floating of exchanger particles, true density should be more than 1. The true density of commercial exchangers is generally between 1.1 to 1.5 g·mL⁻¹.

Apparent density (D_{col}): For apparent density measurements, exact weight of exchanger is taken in a calibrated glass column. After backwashing, water is drained and exchanger material allowed to settle. Apparent density is determined using the equation,

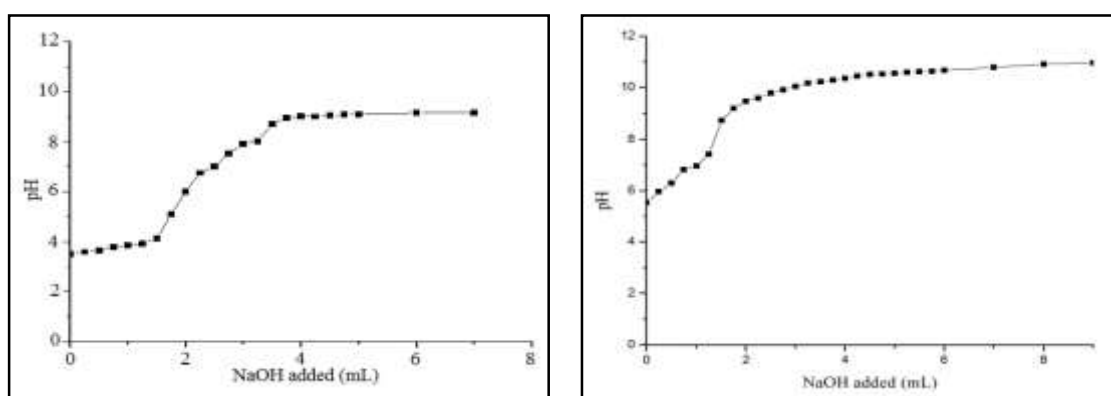
$$\text{Apparent density} = \frac{\text{Weight of ion exchanger}}{\text{Volume of ion exchange bed}} \quad \text{(Eq. 2.3)}$$

True density (D_{ie}): The true density is determined by first weighing specific gravity bottle (*W*). The bottle is weighed again along with the ion exchanger (*W_i*). The bottle is now filled with water along with ion exchange material and weighed (*W_{iw}*). The weight of the specific gravity bottle containing water is also noted (*W_w*). The true density is calculated by using equation,

$$D_{ie} = \frac{(W_i - W)}{(W_w - W_{iw}) + (W_i - W)} \quad \text{(Eq. 2.4)}$$

Nature of exchanger: The nature of exchanger, weak or strong, can be determined by *pH* titration curve. Acid sites in a material can be titrated against an alkali hydroxide (used for neutralization) and a salt solution of same alkali metal (used as a supporting electrolyte). A plot of *pH* versus number of milliequivalents of OH^- ions, is termed as the “*pH* titration curve” or the “potentiometric curve”, which gives an idea regarding the acidic nature of material, weak or strong [40].

500 mg of the material was placed in NaCl (0.1 M, 100 mL) solution. This solution mixture was titrated against NaOH (0.1 M) solution. After addition of every 0.5 mL of titrant, sufficient time was provided for establishment of equilibrium, till the *pH* is constant. A *pH* titration curve is obtained by plotting *pH* versus volume of NaOH/number of milliequivalents of OH^- ions. *pH* titration curves (**Figure 2.1**) indicate that CP and TP are weak cation exchangers.



(a) **(b)**
Figure 2.1 *pH* titration curves of (a) CP and (b) TP

Chemical stability: During ion exchange and regeneration processes, ion exchangers are subjected to a variety of physical and chemical effects. These influences can cause damage to both the exchanger matrix and the functional groups. Oxidants, such as dissolved chlorine in water supplies, react with synthetic ion exchangers to cause a loss of capacity, physical weakening of the exchange material and partial solubilization of the resin. A study of the chemical resistivity/stability of materials in mineral acids, bases and organic solvent media is both useful and important while using the material for various applications in varied environments.

Chemical resistivity/stability in various media - acids (varying concentration of H_2SO_4 , HNO_3 , HCl), bases (varying concentration of NaOH and KOH) and organic

solvents (ethanol, propanol, butanol, benzyl alcohol, 2-ethyl 1-hexanol, benzene, acetone, cyclohexane, toluene, xylene and acetic acid) was studied by taking 500 mg of the material in 50 mL of the particular medium and allowing to stand for 24 h. The change in colour, nature, weight as well as solubility was observed. Further, to confirm the stability/solubility of the material in particular media, supernatant liquid was checked qualitatively for respective elements (*viz* Ce^{4+} , Th^{4+} and PO_4^{3-}) of the material. Maximum tolerable limits evaluated in a particular medium have been presented in **Tables 2.4 and 2.5**. In general, CP and TP are stable in acids and organic solvent media but not so stable in base medium.

2.5.2 Ion Exchange Characteristics

Ion exchange characteristics include ion exchange capacity, effect of calcination on CEC, void volume fraction/porosity, concentration of fixed ionogenic groups, volume capacity of the resin, etc. (**Tables 2.4 and 2.5**)

Cation Exchange Capacity (CEC): Capacity in general can be described as a measure of the quantity of ions, acid or base, removed/exchanged by an ion-exchange material. Capacity and related data are primarily used for two purposes (a) for the characterization of ion exchange materials (b) for use in numerical calculations of ion exchange-operations. The term ion exchange capacity is intended to describe the total available exchange capacity of an ion exchanger, as described by the number of functional groups on it. This value is constant for a given ion exchange material and is expressed in milli equivalents per gram, based on dry weight of material in given form (such as H^+ or Cl^-). For the characterization of ion exchangers, two capacity parameters are commonly used: the total static exchange capacity (which is determined by batch method) and dynamic exchange capacity (which is determined by column method). The exchange capacity depends on the functional groups per gram of exchanger, while the extent of the total exchange capacity depends on the level of ionization of the functional groups of the exchanger and on the chemical and physical conditions of the process. Likewise it is recommended to use sodium acetate for weak acid ion exchangers, NaCl for neutral ion exchangers and NH_4Cl for acidic ion exchangers, for the determination of CEC. The Na^+CEC of materials is generally determined by the column method [41, 42], by varying concentration and volume of electrolyte solution at a fixed flow rate to find optimum concentration and volume required for complete exchange.

In the present study, the Na⁺cation exchange capacity (CEC) of ion exchangers CP and TP were determined by the column method [41, 42] by optimizing volume and concentration of sodium acetate solution (**Figure 2.2**).

Firstly, a fixed volume (250 mL) of sodium acetate solution of varying concentration (0.1 M, 0.2 M, 0.3 M, 0.4 M, 0.5 M, 0.6 M, 0.7 M) was passed through a glass column (30 cm × 1 cm internal diameter) containing 0.5 g of the exchanger, maintaining a flow rate of 0.5 mL·min⁻¹ and effluent (containing H⁺ ions eluted out) titrated against 0.1 M NaOH solution. The optimum concentration of eluent is thus determined. Now, eluent of optimum concentration was used and 10 mL fractions passed through the column maintaining a flow rate 0.5 mL·min⁻¹. This experiment was conducted to find out the minimum volume necessary for a complete elution of the H⁺ ions, which reflects the efficiency of the column. Using these optimized parameters Na⁺ CEC was determined, using the formula aV/W , where a is molarity, V the amount of alkali used during titration, and W is the weight of the exchanger. The CEC values for CP and TP are presented in **Tables 2.4 and 2.5**.

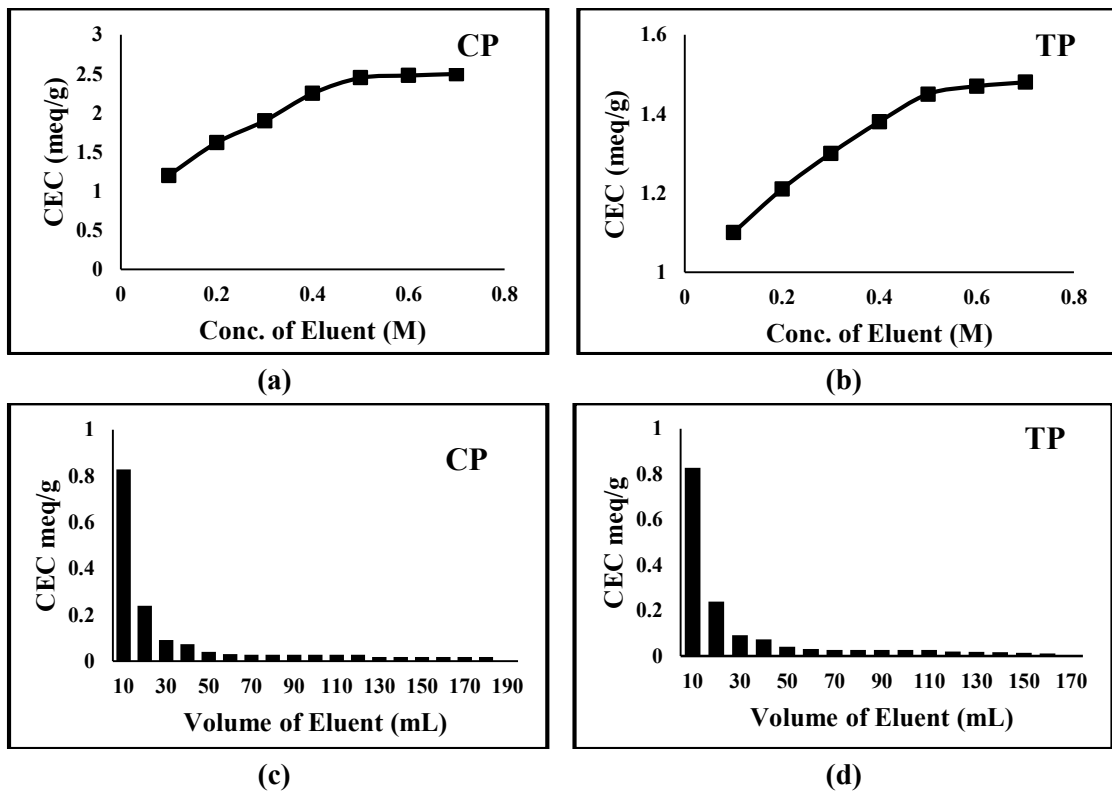


Figure 2.2 Concentration (a & b) and volume (c & d) optimization of eluent for determination of CEC

Effect of calcination on CEC: There are several important ion exchange processes that occur at high temperatures. For such cases, thermal stability is one of the most important requirements of a good ion exchanger. The exchanger in use should be able to withstand the temperature of the reaction system. Ion-exchange materials should not be used at temperatures above those recommended by the manufacturer. Functional groups are lost from both cation- and anion- exchange resins, when the temperature limit is exceeded. The rate of weight loss increases exponentially as the temperature rises above the upper limit.

A study on the effect of calcination on the exchanger material, would give information regarding utility of the material for high temperature applications. The effect of calcination on CEC was studied using 1 g of each sample, calcined in the temperature range 100 °C - 500 °C at an interval of 50 °C for 2 h, cooled to room temperature in desiccator and CEC determined by the column method [39, 40]. The values of Na⁺CEC of calcined samples of CP and TP are presented in **Tables 2.4 and 2.5**.

The Na⁺CEC of the calcined samples shows an initial increase in the CEC value at 100°C which is attributed to loss of moisture adhered to it, thereby increasing the active exchanger content for same weight of material taken for CEC determination. Decrease in CEC beyond 100°C could be attributed to the condensation of structural hydroxyl groups. CEC values are retained upto 150°C.

Void volume fraction/porosity:The porosity of an ion exchanger is related to the degree of cross-linking and the network formed as a result. The porosity also influences ion exchange properties, particularly the capacity and selectivity. The capacity would be much lower than it really is, if the exchanger had no porous structure and if only the functional groups at the surface were active for ion exchange. The high ion exchange capacity obtained in case of porous materials, is due to active functional groups located in the interior of the pores also. Ion-exchange materials are generally microporous or macroporous. Microporous materials are more commonly referred to as gel or gel type exchanger. Porosity in such materials cannot be measured by standard techniques. Such exchanger particles swell with water or a solvent. There is no porosity when the material is dry. Macroporous materials have a measurable porosity which does not disappear when the exchanger is dry. Porosity of the materials has been measured using mercury porosimeter which is discussed in instrumental methods of characterization. Void volume fraction, concentration of fixed

ionogenic group (C_r) and volume capacity of the resin (Q) are calculated using following equations,

Void volume fraction

$$\text{Void volume fraction} = 1 - \frac{D_{col}}{D_{ie}} \quad (\text{Eq. 2.5})$$

Concentration of fixed ionogenic group (C_r)

$$C_r = \frac{D_{ie} \times (100 - \% \text{ moisture}) \times IEC}{100} \quad (\text{Eq. 2.6})$$

Volume capacity of the resin (Q)

$$Q = (1 - \text{void volume fraction}) \times C_r \quad (\text{Eq. 2.7})$$

2.5.3. Instrumental Methods of Characterization

Elemental analysis: In the present study, elemental analysis was performed on ICP-AES spectrometer (Labtam, 8440 Plasmalab). The concentration of different elements measured at ppm level, is converted into the % weight of the element, by incorporating the dilution factor. These values are then converted into moles of each element.

Energy dispersive X-ray analysis (EDX): EDX of the samples were scanned on Jeol JSM-5610-SLV scanning electron microscope. EDX has been used in coordination with and as supportive analysis with ICP-AES which is more accurate compared to EDX.

Elemental analysis performed by ICP-AES, for CP shows % Ce = 33.15; % P = 15.11 and for TP, % Th = 35.10; % P = 9.40 with ratio of Metal:P as 1:2. This is well supported by EDX (**Figure 2.3a**) for CP which shows atomic % of Ce and P to be 34.95% and 65.05% respectively while (**Figure 2.5a**) for TP which shows atomic % of Th and P to be 35.75% and 64.25% respectively.

Thermal analysis: TGA was performed on a Shimadzu, DT-30 thermal analyzer at a heating rate of 10°C per minute. Thermal behaviour of several TMA salts have been investigated and generally examined for loss of moisture ~80 °C, loss of external water molecules ~100-180 °C and for condensation of the structural hydroxyl groups ~180-500 °C and above [41, 42]. TGA of CP and TP presented in **Figures 2.3b and 2.5b** respectively reveals that CP exhibits the first weight loss ~13 % in the temperature range ~30-120 °C and the second weight loss ~8 % in the temperature range 120-500 °C while TP exhibits the first weight loss ~11 % (~30-120 °C) and the second weight loss ~9 % (120-500 °C). The first weight loss in the temperature range ~30-120 °C is attributed to loss of moisture/hydrated water while the second weight

loss in the range 120-500 °C is attributed to condensation of structural hydroxyl groups.

DSC of CP and TP (**Figures 2.3c and 2.5c** respectively) was performed on a Shimadzu, DSC-50 analyzer. An endothermic peak at ~128 °C and 133 °C for CP and TP respectively is observed, attributed to loss of moisture/hydrated water.

Fourier Transform Infrared Spectroscopy (FTIR): FTIR spectra for CP and TP (**Figures 2.3d and 2.5d** respectively) were obtained using KBr wafer on a Shimadzu (Model 8400S). The FTIR spectra of CP and TP exhibits a broad band in the region ~3400 cm⁻¹ which is attributed to asymmetric and symmetric -OH stretching vibration due to residual water and presence of structural hydroxyl groups, H⁺ of the -OH being Brønsted acid sites in nature. These bands indicate the presence of structural hydroxyl groups/catalytic sites in the materials. These sites are also referred to as defective P-OH groups [43]. A sharp medium band at ~1630 cm⁻¹ is attributed to aquo H - O - H bending [44]. The band at ~1050 cm⁻¹ is attributed to P=O stretching while the bands at ~620 cm⁻¹ and ~500 cm⁻¹ is attributed to Metal-O stretching [45].

In general, CEC values decrease on calcination, due to loss of moisture/hydrated water and condensation of structural hydroxyl groups at higher temperatures (**Tables 2.4 and 2.5**). This fact is also evident from the FTIR spectra of the calcined CP and TP (**Figures 2.3e and 2.5e** respectively). It is seen that the intensities of the peaks at -3400 cm⁻¹ and -1638 cm⁻¹ corresponding to the -OH group diminish as temperature increases.

X-ray diffraction studies: XRD was performed on an X-ray diffractometer (Bruker AXS D8) using Cu-K_α radiation (X-ray source of wavelength 1.5418 Å) with a nickel filter. The absence of sharp peaks in the X-ray diffractograms of CP and TP (**Figures 2.4a and 2.6a** respectively), and CP_M and TP_M (**Figures 2.4b and 2.6b** respectively) indicates amorphous nature of all the materials.

Scanning electron microscopy (SEM): SEM was scanned on Jeol JSM-5610-SLV scanning electron microscope. SEM images of CP, CP_M, TP and TP_M are presented in **Figures 2.4c, 2.4d, 2.6c and 2.6d** respectively. Variation in surface morphology as well as irregular particle size of CP, TP, CP_M and TP_M also indicate amorphous nature.

Based on the elemental analysis (ICP–AES) and thermal analysis (TGA) data, CP and TP, are formulated as Ce(HPO₄)₂·5H₂O and Th(HPO₄)₂·6H₂O. The number of

water molecules in each case is calculated using Alberti and Torracca (1968) formula [46].

2.5.4. Catalyst Characterization

Surface area determination (BET method): Adsorption desorption isotherms of Nitrogen (N₂) was recorded by BET (Braunauer Emmett Teller) multipoint method using a Micromeretics Gemini 2220 series surface area analyzer, at -196 °C after degassing the sample at 300 °C for 4 h. The surface area values and pore diameter of CP, TP, CP_M and TP_M are presented in **Tables 2.4 and 2.5**.

Surface acidity determination (NH₃-TPD method): Surface acidity was determined on Chemisorb 2720, by a temperature programmed desorption (TPD) of ammonia. All materials were preheated at 150°C, 200°C and 700°C temperatures. Ammonia was chemisorbed at 120°C and then desorption was carried out upto 700°C at a heating rate of 10 °C·min⁻¹ in all cases {**Figures 2.4(e-f) and 2.6(e-f)**}.

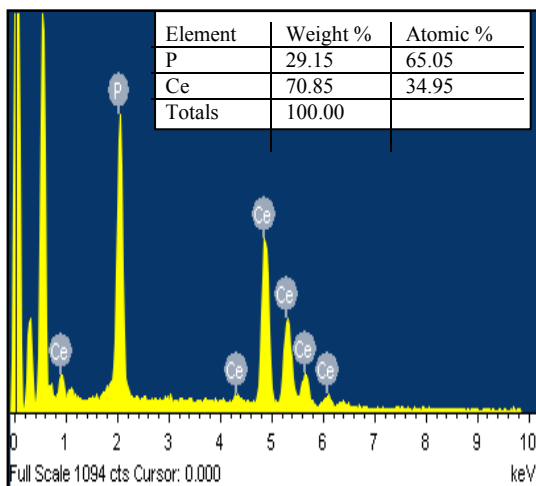
As already discussed earlier in the text, acidity in CP and TP is due to the presence of structural hydroxyl protons, H⁺ of the –OH being the Brønsted acid sites. Further, surface acidity values of CP and TP depend on the size and charge of the cation. Smaller size and higher charge of the cation indicates greater tendency to release a proton, i.e. H⁺ of the –OH groups present in CP and TP. In the present study Ce⁴⁺ and Th⁴⁺, both ions being tetravalent as well as bearing common anion PO₄³⁻, size of the cation Ce⁴⁺ (1.05 Å) and Th⁴⁺ (1.08 Å) seems to play a dominant role. The acidity in the materials follows the order CP > TP and CP_M > TP_M (**Table 2.6**). Decrease in surface acidity for CP and TP with increasing preheating temperatures could be attributed to condensation of structural hydroxyl groups as discussed above in thermal behavior of these materials. This is well supported by CEC values, which reflect on the protonating ability and thus the acidity of the materials [48]. CEC values also decreases with increasing calcination/preheating temperature has already been discussed in FTIR spectra of calcined CP and TP (**Figures 2.3e and 2.5e** respectively).

Table 2.4 *Characterization of CP*

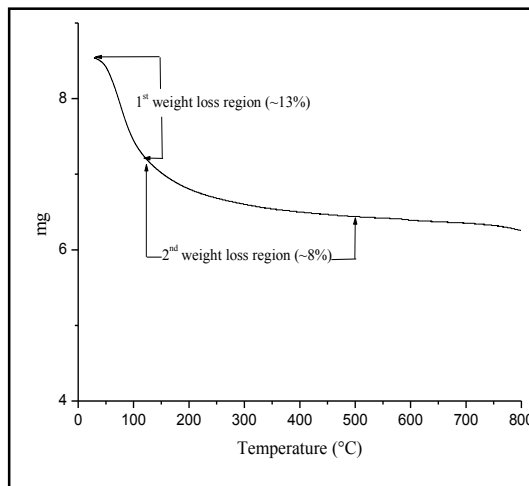
| |
|---|
| Physico-chemical and Ion Exchange Characterization |
|---|

Chapter 2 - Synthesis and Characterization of CP and TP

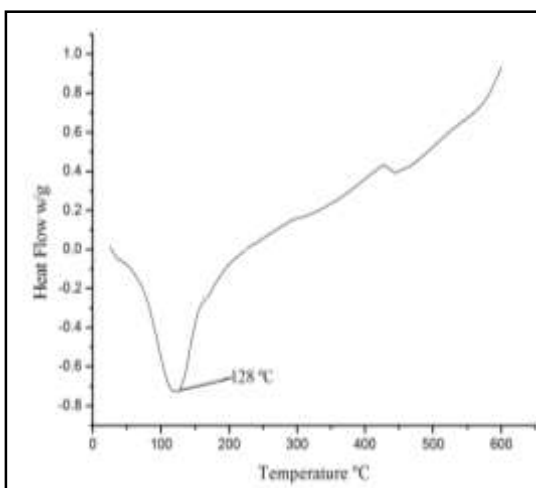
| | | | | | |
|---|---|--|---------------------------|--|----------------------------|
| Appearance | Yellow hard granules | Cation exchange capacity(CEC) and effect of calcination on CEC | | Temperatures (°C) | CEC (meq.g ⁻¹) |
| Particle size | 250-590 μ | | | RT | 2.45 |
| % Moisture content | 10.26 % | | | 100 | 2.20 |
| True density | 2.86 g·mL ⁻¹ | | | 200 | 2.08 |
| Apparent density | 0.60 g·mL ⁻¹ | | | 300 | 1.61 |
| Void volume fraction | 0.79 | | | 400 | 0.70 |
| Concentration of fixed ionogenic group | 6.28 mmol·g ⁻¹ | | | 500 | 0.15 |
| Volume capacity of resin | 1.31 mL·g ⁻¹ | Chemical Stability (Maximum tolerable limits) | Acids | 3N H ₂ SO ₄ , 3N HNO ₃ , 5HCl | |
| Nature of exchanger | Weak cation exchanger | | Bases | 0.5 N NaOH, 0.5 N KOH | |
| | | | Organic Solvents | Ethanol, Acetone, Toluene, Acetic Acid, Benzene, Xylene | |
| Instrumental Methods of Analysis | | | | | |
| Elemental Analysis | | | Elements | | |
| | ICP-AES (%) | | Ce(IV) = 33.15 | P = 15.11 | |
| | EDX analysis (atomic %) | | Ce(IV) = 34.95 | P = 65.05 | |
| FTIR | Peaks (cm ⁻¹) | | ~3400 | ~1630 | ~1050 |
| | Groups assigned | | -OH _{stretching} | H-O-H _{bending} | P=O _{stretching} |
| TGA | Temperature range(°C) | | 30-100 | | |
| | % Weight loss | | ~11 % | | |
| | Temperature range(°C) | | 120-500 | | |
| | % Weight loss | | ~9 % | | |
| DSC | Endothermic peak | | ~128 °C | | |
| XRD | Nature of materials (CP & CP _M) | | Amorphous | | |
| SEM | Size of particles (CP & CP _M) | | Irregular | | |
| Catalyst Characterization | | | | | |
| Surface area (m ² .g ⁻¹) | CP | | 20.71 | | |
| | CP _M | | 1.40 | | |
| Average Pore diameter(nm) | CP | | 2.74 | | |
| | CP _M | | 2.20 | | |
| Pore Volume (mL·g ⁻¹) | CP | | 0.014 | | |
| | CP _M | | 0.013 | | |



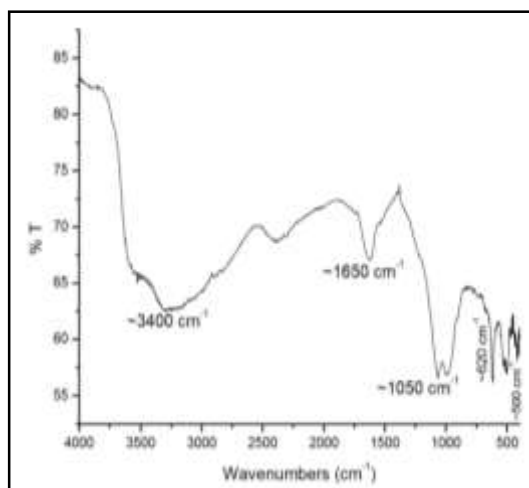
(a)



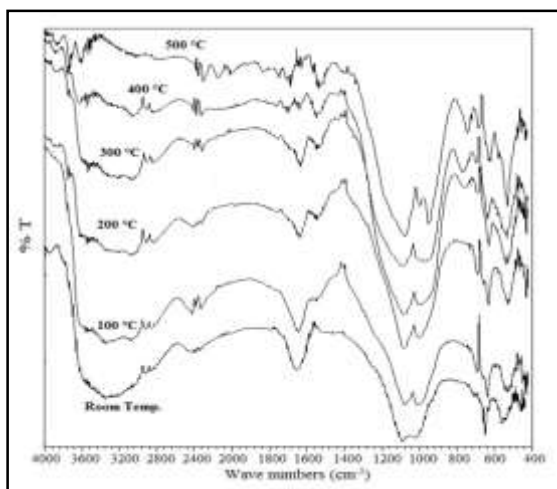
(b)



(c)



(d)



(e)

Figure 2.3 (a)EDX of CP (b) TGA of CP (c) DSC of CP, (d) FTIR spectrum of CP and (e) FTIR spectra of calcined CP

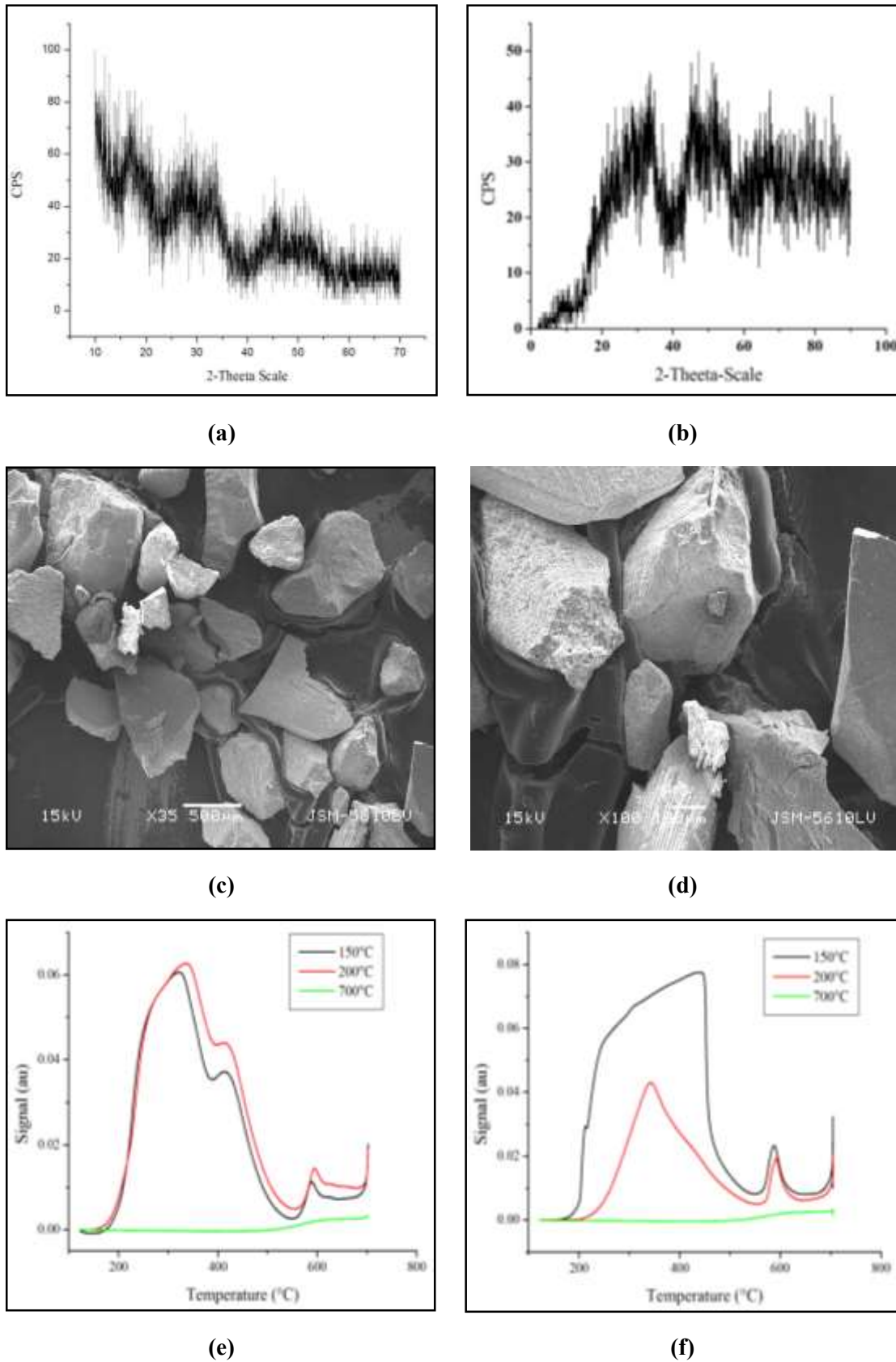
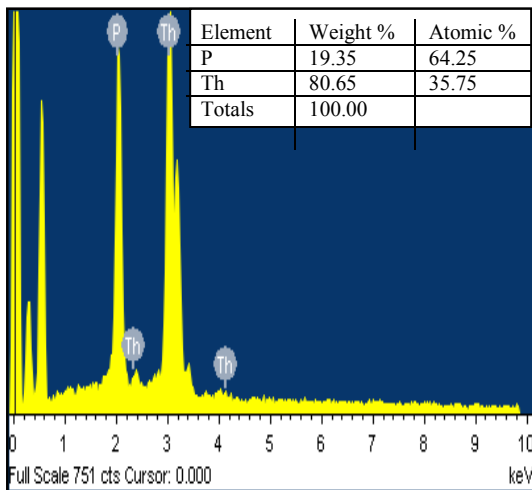


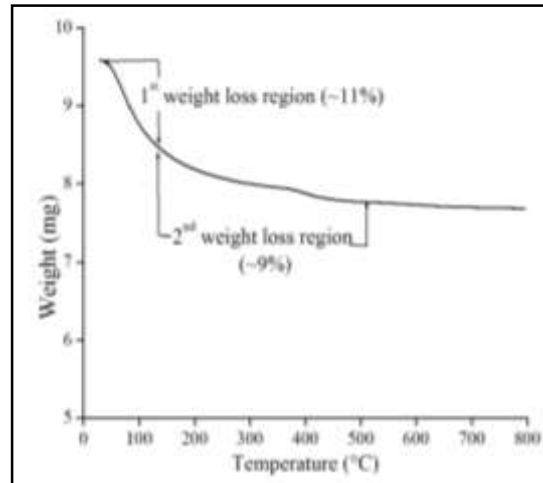
Figure 2.4 (a) XRD of CP, (b) XRD of CP_M, (c) SEM of CP, (d) SEM of CP_M, (e) NH₃-TPD curve for CP and (f) NH₃-TPD curve for CP_M

Table 2.5 Characterization of TP

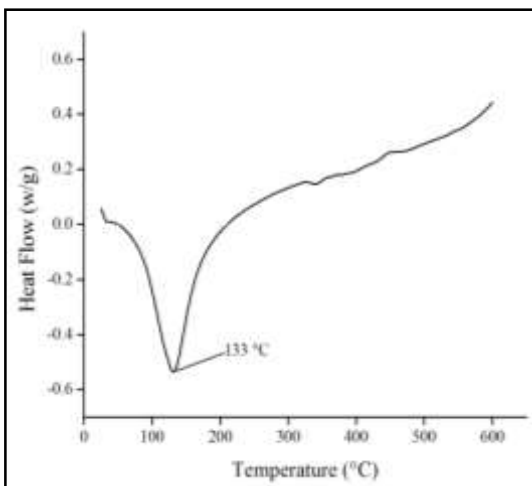
| Physico-chemical and Ion Exchange Characterization | | | | |
|---|---|--|---------------------------|--|
| Appearance | White hard granules | Cation exchange capacity(CEC) and effect of calcination on CEC | Temperatures (°C) | CEC (meq.g ⁻¹) |
| Particle size | 250-590 μ | | RT | 1.48 |
| % Moisture content | 8.07 % | | 100 | 1.39 |
| True density | 2.98 g·mL ⁻¹ | | 200 | 0.46 |
| Apparent density | 1.50 g·mL ⁻¹ | | 300 | 0.28 |
| Void volume fraction | 0.88 | | 400 | 0.16 |
| Concentration of fixed ionogenic group | 6.52 mmol·g ⁻¹ | | 500 | 0.10 |
| Volume capacity of resin | 3.23 mL·g ⁻¹ | Chemical Stability (Maximum tolerable limits) | Acids | 1N H ₂ SO ₄ , 2N HNO ₃ , 3HCl |
| Nature of exchanger | Weak cation exchanger | | Bases | 0.5 N NaOH, 0.5 N KOH |
| | | | Organic Solvents | Ethanol, Acetone, Toluene, Acetic Acid, Benzene, Xylene |
| Instrumental Methods of Analysis | | | | |
| Elemental Analysis | | | Elements | |
| | ICP-AES (%) | | Th (IV) = 35.10 | P = 9.40 |
| | EDX analysis (atomic %) | | Th (IV) = 35.75 | P = 64.25 |
| FTIR | Peaks (cm ⁻¹) | | ~3400 | ~1630 |
| | Groups assigned | | -OH _{stretching} | H-O-H _{bending} |
| TGA | Temperature range(°C) | | 30-100 | |
| | % Weight loss | | ~13 % | |
| | Temperature range(°C) | | 120-500 | |
| | % Weight loss | | ~8 % | |
| DSC | Endothermic peak | | ~133 °C | |
| XRD | Nature of materials (TP and TP _M) | | Amorphous | |
| SEM | Size of particles (TP and TP _M) | | Irregular | |
| Catalyst Characterization | | | | |
| Surface area (m ² ·g ⁻¹) | TP | | 1.94 | |
| | TP _M | | 1.22 | |
| Average Pore diameter (nm) | TP | | 2.68 | |
| | TP _M | | 2.35 | |
| Pore Volume (mL·g ⁻¹) | TP | | 0.001 | |
| | TP _M | | -- | |



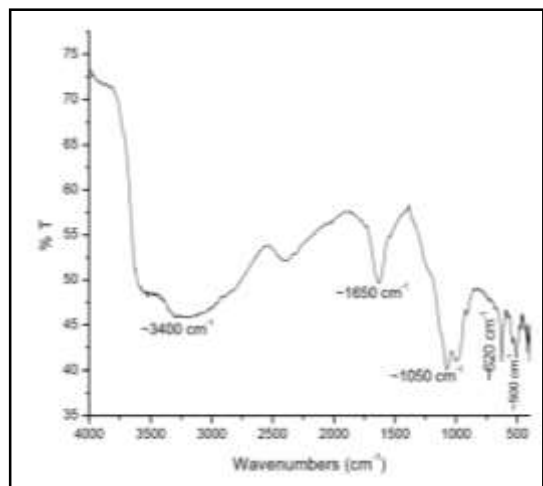
(a)



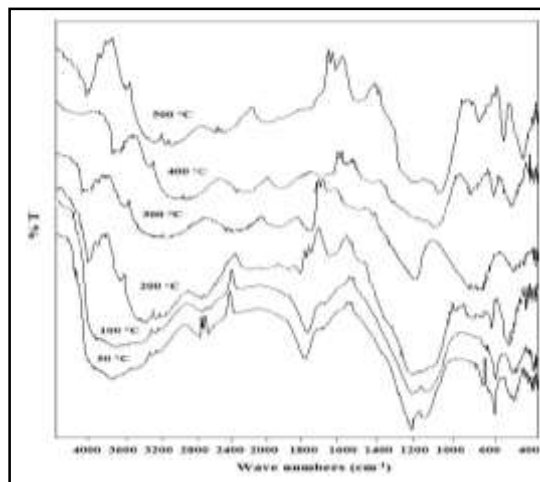
(b)



(c)



(d)



(e)

Figure 2.5(a) EDX of TP, (b) TGA of TP, (c) DSC of TP, (d) FTIR spectrum of TP and (e) FTIR spectra of calcined TP

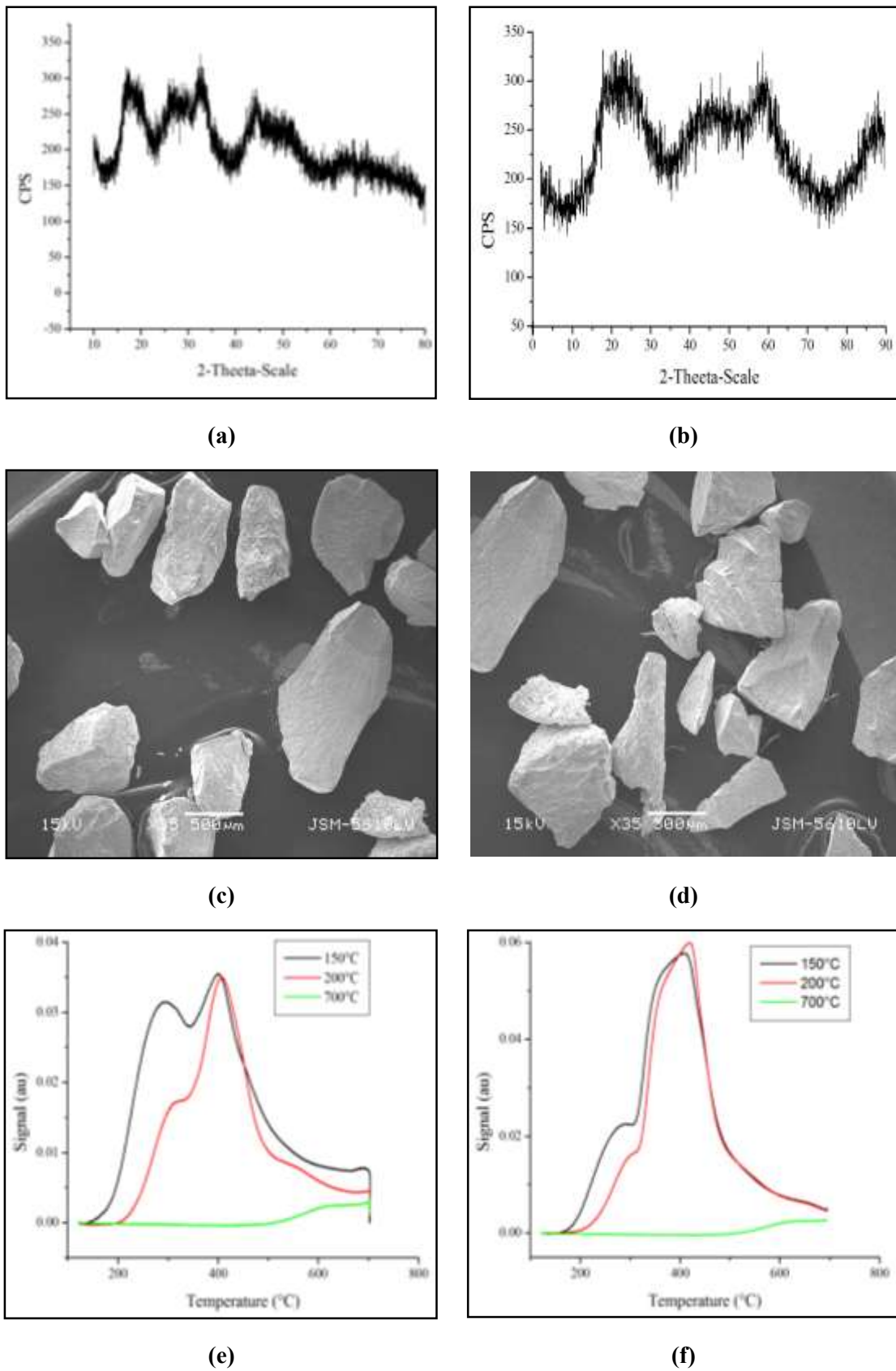


Figure 2.6(a)XRD of TP, (b) XRD of TP_M, (c) SEM of TP, (d) SEM of TP_M,(e) NH₃-TPD curve for TP and (f) NH₃-TPD curve for TP_M

Table 2.6 Surface acidity and CEC values at 150, 200 and 700 °C preheating temperatures

| Samples | Calcination/preheating Temperature (°C) | Total acidity (NH ₃ -TPD method) (mmol·g ⁻¹) | CEC (meq·g ⁻¹) |
|-----------------|---|---|----------------------------|
| CP | 150 | 0.95 | 2.04 |
| | 200 | 0.89 | 1.89 |
| | 700 | -- | -- |
| CP _M | 150 | 1.26 | 2.20 |
| | 200 | 0.45 | 2.00 |
| | 700 | -- | -- |
| TP | 150 | 0.78 | 0.70 |
| | 200 | 0.50 | 0.46 |
| | 700 | -- | -- |
| TP _M | 150 | 0.80 | 0.92 |
| | 200 | 0.76 | 0.70 |
| | 700 | -- | -- |

2.6 CONCLUSIONS

The present work is focused towards synthesis and characterization of amorphous CP and TP and their applications as cation exchangers, solid acid catalysts and solid state proton conductors. Amorphous materials are preferred [49] to crystalline materials as they can be obtained in a range of mesh sizes suitable for column operations. Crystalline materials have shown the disadvantage of small grain size, restricting their application in column operation. Further, it is observed that both surface area and surface acidity decreases with increasing crystallinity of the material [49].

In **Chapter I** of the thesis, the structural aspects of crystalline CP and TP have been discussed in details available in literature. Reports[50-56] on structure elucidation of amorphous materials reveal that focus was largely on zirconium (IV) phosphate (ZrP). Based on these reports [50-56], the following structures could be predicted for CP and TP {given as **Figures 2.7(a-e)**}, wherein the H⁺ of the structural -OH groups are the exchangeable protons, which is confirmed by several characterization studies discussed earlier in text.

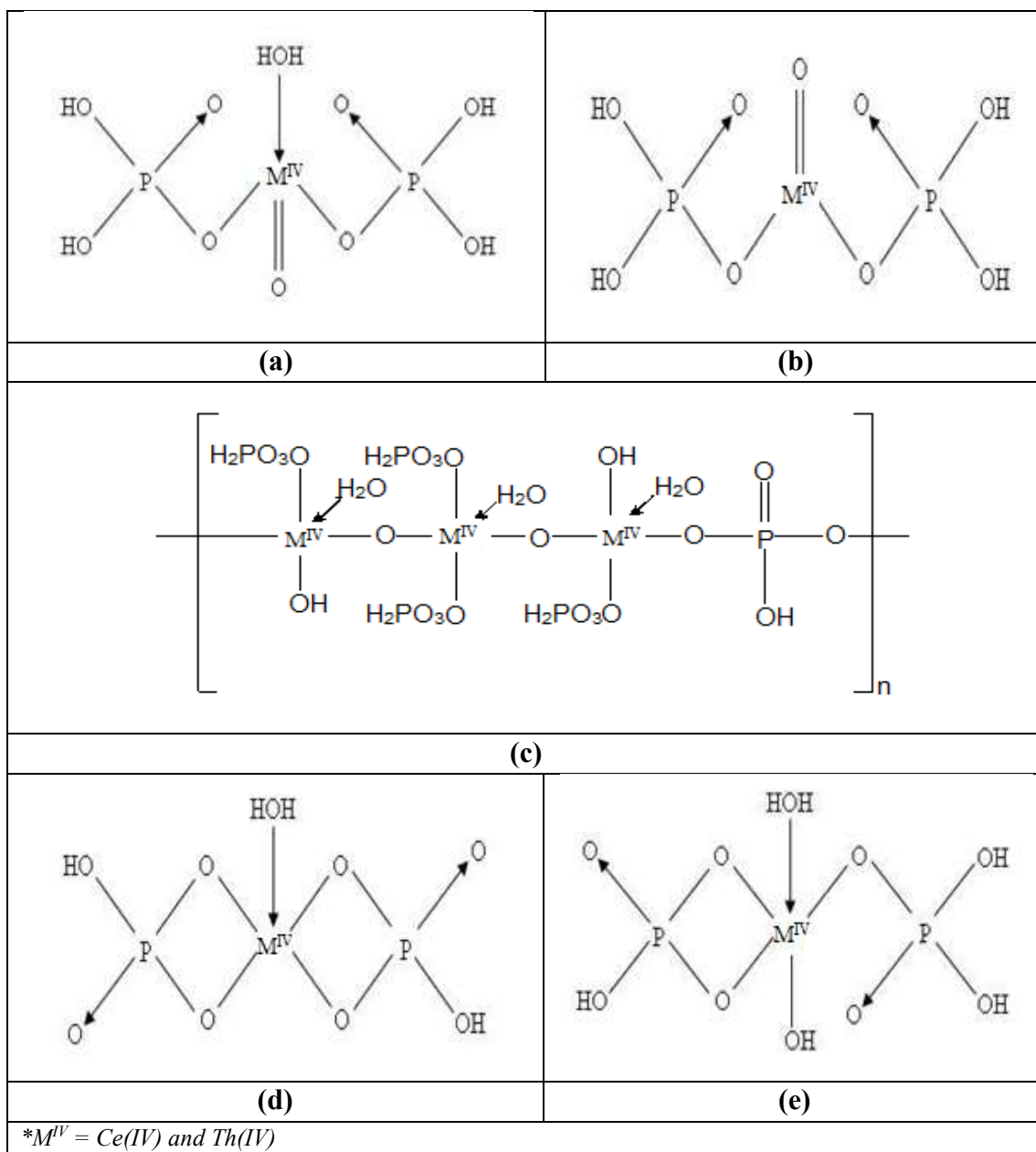


Figure 2.7(a-e) Proposed structures for CP and TP

A broad band in the region $\sim 3400\text{ cm}^{-1}$ {FTIR spectra - **Figures 2.3d** (CP) and **2.5d** (TP)} is attributed to symmetric and asymmetric -OH stretching vibrations, while band at $\sim 1635\text{ cm}^{-1}$ is attributed to aquo (H-O-H) bending [43]. These bands indicate the presence of structural hydroxyl groups, H⁺ of the -OH being cation exchange sites/Brønsted acid sites in nature [44]. The presence of cation exchange sites is more evident from the Na⁺CEC value that has been determined – found to be 2.45 and 1.48 meq·g⁻¹ for CP and TP respectively. CEC values decrease with increasing temperatures, attributed to loss of moisture/hydrated water and

condensation of structural hydroxyl groups. This fact is also evident from the FTIR spectra of calcined CP and TP (**Figures 2.3e and 2.5e** respectively). It is seen that the intensities of the peaks at -3400 cm^{-1} and -1638 cm^{-1} corresponding to the -OH group diminish as temperature increases [41].

pH titration curve - a plot of pH versus number of milliequivalents of OH^- ions {**Figure 2.1(a-b)**}, shows that both CP and TP are weak cation exchangers. A study on chemical stability shows that both CP and TP are found to be stable in acids and organic solvent media but not so stable in base medium.

Thermal analysis (TGA) exhibits two weight loss regions {**Figures 2.3b(CP) and 2.5b(TP)**}. The first weight loss (upto $\sim 120\text{ }^\circ\text{C}$) is attributed to loss of moisture / hydrated water while the second weight loss in the range $120 - 500\text{ }^\circ\text{C}$ is attributed to condensation of structural hydroxyl groups.

Absence of sharp/characteristic peaks in X-ray diffractogram of CP {**Figure 2.4(a-b)**} and TP {**Figure 2.6(a-b)**} indicates that the materials are amorphous in nature. Variation in surface morphology as well as irregular particle size of CP and TP also indicate amorphous nature {SEM images **Figures 2.4(c-d) and 2.6(c-d)**}.

Based on physico-chemical, ion exchange and instrumental methods of characterization, it can be concluded that both CP and TP exhibit promising ion exchange characteristics - good CEC value (retained upto $150\text{ }^\circ\text{C}$), granular nature (30-60 mesh size) suitable for column operation, good chemical (insoluble in aqueous, acid and organic solvent media) and thermal stability. Evaluation of surface acidity (retained upto $150\text{ }^\circ\text{C}$) indicates good potential for CP and TP to be used as environment friendly solid acid catalysts and as solid state proton conductors.

REFERENCES

1. Alberti G, Constantino U, DiGregorio F, Galli P, Torracca E, Crystalline insoluble salts of polybasic metals - III: Preparation and ion exchange properties of cerium(IV) phosphate of various crystallinities, *J. Inorg. Nucl. Chem.*, **1968**, 30, 295-301.
2. Alberti G, Constantino U, Crystalline insoluble acid salts of tetravalent metals X. Fibrous thorium phosphate, a new inorganic ion-exchange material suitable for making, (support-free) inorganic sheets, *J Chromatog.*, **1970**, 50, 482-486.
3. Alberti G, Constantino U, Zsinka L, Crystalline insoluble acid salts of tetravalent metals - XII: Synthesis and ion-exchange properties of microcrystalline cerium(IV) phosphate *J. Inorg. Nucl. Chem.*, **1972**, 34, 3549.
4. Hartley W N, *J. Chem. Soc.*, **1882**, 41, 202.
5. Cilley W A, Ph.D. Dissertation, University of Wisconsin, Madison (**1963**).
6. König K H, Meyn E, Amorphous and crystalline cer(IV) phosphate als ionenaustauscher-I: Herstellung and chemische Eigenschaften, *J. Inorg. Nucl. Chem.*, **1967**, 29, 1153-1160
7. König K H, Meyn E, Amorphe und kristalline cer(IV)-phosphate als ionenaustauscher-II: Ionenaustauschereigenschaften gegenüber einwertigen *J. Inorg. Nucl. Chem.* **1967**, 29, 1519-1526
8. König K H, Eckstein G, Amorphe und kristalline cer(IV)-phosphate als ionenaustauscher-III Herstellung, chemische und kationenaustauschereigenschaften kristalliner cerium (IV)-phosphat-sulfate, *J. Inorg. Nucl. Chem.*, **1969**, 31, 1179- 1188
9. König K H, Eckstein G, Amorphe und kristalline cer(IV)-phosphate als ionenaustauscher-IV Makrosorption, Tracersorption und Nuklidtrennungen an kristallinen cerium (IV)-phosphatsulfaten, *J. Inorg. Nucl. Chem.*, **1972**, 34, 3771-3779.
10. Larsen E M, Cilley W A, The exchange of Li⁺, Na⁺ and K⁺ on cerium(IV) phosphate, *J. Inorg. Nucl. Chem.*, **1968**, 30, 287-293.
11. Hermant R G, Clearfield A, Crystalline cerium(IV) phosphates – II: The ion exchange characteristics with alkali metal ions, *J Inorg. Nucl. Chem.*, **1976**, 38, 853-858

12. Hikichi Y, Nomura T, Tanimura Y, Suzuski S, Miyami, Sintering and properties of monazite-type CePO_4 , *J. Am. Ceram. Soc.* **1990**, 73 (12), 3594
13. Onoda H, Narini H, Maki H, Motooka I, Syntheses of various rare earth phosphates from some rare earth compounds, *Mater. Chem. Phys.*, **2002**, 73, 19-23.
14. Ruigang W, Wei P, Jain C, Minghao F, Zhenzhu C, Yongming L, *Mater. Chem. Phys.* **2002**, 9666, 1.
15. Rajesh K, Mukundan P, Krishna Pillai, Nair V R, Warriar K G K, High-surface-area nano-crystalline cerium phosphate through aqueous sol-gel route, *Chem. Mater.*, **2004**, 16, 2700-2705.
16. Yang R, Qin J, Li M, Liu Y, Li F, Redox hydrothermal synthesis of cerium phosphate microspheres with different architectures, *Cryst. Eng. Comm.*, **2011**, 13, 7284-7292.
17. Bao J, Yu R, Zhang J, Yang X, Wang D, Deng J, Chen J, Xing X, Low-temperature hydrothermal synthesis and structure control of nano-sized CePO_4 , *Cryst. Eng. Comm.*, **2011**, 11, 1630-1634..
18. Brandel V, Clavier N, Dacheux N, Synthesis and characterization of uranium (IV) phosphate-hydrogenphosphate hydrate and cerium (IV) phosphate-hydrogenphosphate hydrate, *J Solid State Chem.*, **2005**, 178(1), 1054-1063.
19. Shakshooki S K, Elejmi A A, Hamassi A M, El-Akari E A, Masoud N A, Facile synthesis of poly (vinylalcohol)/fibrous cerium phosphate nano-composite membranes, *Phys. Mater. Chem.*, **2014**, 2(1), 1-6.
20. Ekthammathat N, Phuruangrat N, Thongtem T, Thongtem S, Facile hydrothermal synthesis and optical properties of monoclinic CePO_4 nanowires with high aspect ratio, *J. Nanomater.*, **2012**, 1-6.
21. Nazary M, Wallez G, Chaneac C, Tronc E, Ribot F, Quarton M, Jolivet J P, Synthesis and characterization of $\text{Ce}^{\text{IV}}(\text{PO}_4)(\text{HPO}_4)_{0.5}(\text{H}_2\text{O})_{0.5}$, *J Phys. Chem. Solids.*, **2006**, 67, 1075-1078.
22. Hanna A A, Mousa S M, Elkomy G M, Sherief M A, Synthesis and microstructure studies of nanosized cerium phosphates, *Eur. J. Chem.*, **2010**, 1(3), 211-215.
23. Brandel V, Clavier N, Dacheux N, Rousselle J, Genet M, Synthesis of new thorium phosphates, *C. R. Chemie.*, **2002**, (5), 599-606.

24. Brandel V, Dacheux N, Genet M, Podor R, Hydrothermal synthesis and characterization of the thorium phosphate hydrogenphosphate, Thorium hydroxide phosphate, and dithorium oxide phosphate, *J Solid State Chem.*, **2001**, 159, 139-148.
25. Brandel V, Clavier N, Dacheux N, Querton M, Wouter van B, From thorium phosphate hydrogenphosphate hydrate to β -thorium phosphate diphosphate: structural evolution to a radwaste storage ceramic, *J Solid State Chem.*, **2006**, 179, 3007-3016.
26. Brandel V, Clavier N, Dacheux N, Querton M, Bregiroux D, Negative thermal expansion in $\text{Th}_2\text{O}(\text{PO}_4)_2$, *Mater. Res. Bull.*, **2011**, 1777-1780.
27. Tananaev I V, Rozanov I A, Beresnev E N, Studies on the chemistry of uranium and thorium phosphates, *Inorg. Mater.*, **1976**, 12, 748-760.
28. De A K, Chowdhury K, Studies on thorium phosphate ion exchanger II distribution coefficient measurements and selective Ion-exchange separations of some metal ions, *J Chromatog.*, **1974**, 101, 73-78.
29. Rawat D, Dash S, Joshi A R, Thermodynamic studies of thorium phosphate diphosphate and phase investigations of Th-P-O and Th-P-H₂O systems, *Thermochimica Acta*, **2014**, 581, 1-13.
30. Varshney K G, Agrawal A, Mojumdar S C, Pyridine based thorium (IV) phosphate hybrid exchanger: Synthesis, characterization and thermal behavior, *J Therm. Ana. Calor.*, **2007**, 90(3), 721-724.
31. Varshney K G, Tayal N, Polystyrene thorium (IV) phosphate as a new crystalline and cadmium selective fibrous ion exchanger. Synthesis, characterization and analytical applications, *Langmuir*, **2001**, 17, 2589-2593.
32. Varshney K G, N Tayal, Khan A A, Niwas R, Synthesis, characterization and analytical applications of lead (II) selective polyacrylonitrile thorium (IV) phosphate: a novel fibrous ion exchanger, *Coll. Surf. A: Physicochem. Eng. Aspects*, **2001**, 181, 123-129.
33. Somya A, Varshney K G, Rafiquee M Z A, , Synthesis, characterization and analytical applications of sodium dodecyl sulphate cerium (IV) phosphate: A new Pb (II) selective, surfactant-based intercalated fibrous ion exchanger, *Coll. Surf. A: Physicochem. Eng. Aspects*, **2009**, 336, 142-146.

34. Varshney K G, Agrawal A, Mojumdar S C, Pyridine based cerium (IV) phosphate hybrid exchanger: Synthesis, characterization and thermal behavior, *J Therm. Anal. Calor.*, **2007**, 90(3), 731-734
35. Hiavacek V, Puszynski J, Chemical engineering aspects of advanced ceramic materials, *Ind. Eng. Chem. Res.*, **1996**, 35, 349-377.
36. Bajia S, Sharma R, Bajia B, Solid-state microwave synthesis of melamine-formaldehyde resin, *E J. Chemi.*, **2009**, 6(1), 120-124.
37. Vaidhyanathan B, Balaji K, Rao K J, Microwave-assisted solid-state synthesis of oxide ion conducting stabilized bismuth vanadate phases, *Chem. Mater.* **1998**, 10, 3400-3404
38. Zhang P, Yin S, Satp T, Synthesis of high-activity TiO₂ photocatalyst via environmentally friendly and novel microwave assisted hydrothermal process, *App. Catal. B: Environ.*, **2009**, 89, 118-122.
39. Martinola F, Kune G, *International Conference on Ion Exchange*, London, **1969**.
40. Helfferich F, *Ion Exchange*, McGraw Hill, New York, **1962**.
41. Patel P, Chudasama U, Synthesis and characterization of a novel hybrid cation exchange material and its application in metal ion separations, *Ion Exch. Lett.*, **2011**, 4, 7-15.
42. Thakkar R, Chudasama U, Synthesis and characterization of zirconium titanium phosphate and its application in separation of metal ions, *J. Haz. Mater.*, **2009**, 172, 129-137.
43. Bhaumik A, Inagaki S, Mesoporoustitanium phosphate molecular sieves with ion-exchange capacity, *J Am. Chem. Soc.*, **2001**, 123, 691-696.
44. Seip C T, Granroth G E, Meisel M W, Talham D R, Langmuir-blodgett films of known layered solids: preparation and structural properties of octadecylphosphonate bilayers with divalent metals and characterization of a magnetic langmuir-blodgett film, *J Am. Chem. Soc.*, **1997**, 119, 7084-7094.
45. Nilchi A, Ghanadi M M, Khanchi A, Characteristics of novel types substituted cerium phosphates, *J Radioana. Nucl. Chem.*, **2000**, 245(2), 589-594.
46. Alberti G, Torracca E, Crystalline insoluble acid salts of polyvalent metals and polybasic acids - VI: Preparation and ion-exchange properties of crystalline titanium arsenate, *J Inorg. Nucl. Chem.*, **1968**, 30, 3075-3080.

47. Schmidt R, Stocker M, Hansen E, Akporiaye D, Ellestad O H, MCM-41: a model system for adsorption studies on mesoporous materials, *Micro. Mater.*, **1995**, 3, 443-448.
48. Ghodke S, Chudasama U, Solvent free synthesis of coumarins using environment friendly solid acid catalysts, *App. Catal. A: Gen.*, **2013**, 453, 219-226.
49. Gupta V K, Singh P, Rahman N, Synthesis, characterization and analytical application of zirconium (IV) selenoiodate: a new cation exchanger, *Anal. Bioanal. Chem.*, **2005**, 381, 471-476.
50. Clearfield A, Phosphates, phosphites and phosphonates of groups 4 and 14 metals, *Comments Inorg. Chem.*, **1990**, 10, 89.
51. Amphlett C B, *Inorganic Ion exchangers*, Elsevier, Amsterdam (**1964**).
52. Kraus K A, Phillips H O, Anion exchange Studies. XIX. Anion exchange properties of hydrous zirconium oxide, *J Am. Chem. Soc.*, **1956**, 78 249-249.
53. Clearfield A, Stynes J, The preparation of crystalline zirconium phosphate and some observations on its ion exchange behaviour, *J Inorg. Nucl. Chem.*, **1964**, 26, 117-129.
54. Clearfield A, Smith G D, Crystallography and structure of α -zirconium bis(monohydrogen orthophosphate) monohydrate, *Inorg. Chem.*, **1969**, 8 431-436.
55. Clearfield A, Layered and Three-dimensional phosphates of tetravalent elements, *Eur. J Solid Stat. Inorg. Chem.*, **1991**, 28, 37-42.
56. Slade R C T, Knowels J A, Jones D J, Roziere J, The isomorphous acid salts α -Zr(HPO₄)₂·H₂O, α -Ti(HPO₄)₂·H₂O and α -Zr(HAsO₄)₂·H₂O. Comparative thermochemistry and vibrational spectroscopy, *Solid State Ionics.*, **1997**, 96, 9-19.